**Proceedings of**
**11th European Conference on Turbomachinery Fluid dynamics & Thermodynamics**
**ETC11, March 23-27, 2015, Madrid, Spain**

# FLAT PLATE HONEYCOMB SEALS ACOUSTIC ANALYSIS

*B. Facchini - D. Massini*

Industrial Engineering Department, University of Florence
via di S. Marta 3, 50133 Florence, Italy
daniele.massini@htc.de.unifi.it

*C. Bianchini - M. Micio*

Ergon Research s.r.l.
via Panciatichi 92, 50127 Florence, Italy
mirko.micio@ergonresearch.it

*A. Ceccherini - L. Innocenti*

GE Oil & Gas
via Matteucci 2, 50127 Florence, Italy
alberto.ceccherini@ge.com

**ABSTRACT**

**Honeycomb seals are widely used in centrifugal compressors both for the high leakage flow reduction and the enhanced rotor dynamic stability. Due to the narrow gaps and high rotational speeds the flow inside the honeycomb seals is affected by the onset of acoustic phenomena which is the subject of the present paper.**

**A stationary test rig, composed by a honeycomb surface facing a flat plate, designed to evaluate the friction factor within such type of seals is here used to demonstrate the phenomena leading to friction factor jumps occurring at certain flow speeds.**

**Combined use of static pressure measurements and hot wire anemometry, supported by numerical analysis, permitted to compute the characteristic Strouhal number of the flow above the cavity and to define a corrected Mach number able to represent the air velocities characterized by friction factor jumps. It was also possible to note that the friction factor enhancement occurs when the unsteady forcing due to flow-cavity interaction excites the air system eigenmodes.**

**These findings were generalized for six different honeycomb geometries tested with seven increasing clearances each and for a range of Reynolds number comprised between 40000 and 130000.**

## NOMENCLATURE

$A$ Test rig cross section $[m^2]$
$C$ Cell width $[m]$
$c$ Velocity $[m/s]$
$c_0$ Speed of sound $[m/s]$
$D$ Cell depth $[m]$
$D_h$ Hydraulic diameter $[m]$
$f_f$ Friction factor $[-]$
$H$ Seal clearance $[m]$
$H_0$ Minimum seal clearance $[m]$
$HC$ Honeycomb
$L$ Seal length $[m]$
$\dot{m}$ Mass flow rate $[kg/s]$
$M$ Mach number $[-]$
$Mach_{eff}$ Corrected Mach number $[-]$
$P$ Static pressure $[Pa]$
$p'$ Acoustic pressure $p' = P - \lim_{T\to\infty} \frac{\int_0^\infty P dt}{T}$ $[Pa]$
$R$ Gas constant $[J/(kgK)]$
$Re$ Reynolds number $\frac{D_h \rho c}{\mu}$
$T$ Cell thickness $[m]$
$T_0$ Total temperature $[K]$
$V$ Volume $[m^3]$
$W$ Seal width $[m]$
$X$ Span-wise direction $[-]$
$Y$ Normal direction $[-]$
$Z$ Stream-wise direction $[-]$
$z$ Stream-wise position $[m]$
$\gamma$ Specific heat ratio $[-]$
$\mu$ Dynamic viscosity $[Pas]$
$\rho$ Density $[kg/m^3]$
$\sigma$ standard deviation $[-]$
$\tau_f$ Shear stress due to wall friction $[Pa]$
$SF$ Scale Factor $[-]$
$U_c$ Convection velocity of the vortical structures $[m/s]$

## INTRODUCTION

In centrifugal compressors design, selection and dimensioning of seals have a primary role in reducing leakages and enhancing working pressures and rotational speeds. The presence of very narrow clearances, high pressure and high relative speed motion can however affect the compressor rotor-dynamic stability (Childs and Vance (1997)).

Among the different devices employed in seal gaps to confine the main flow path, honeycomb is particularly performing in terms of improved rotor-dynamic stability. Derived from aircraft engine technology, they can be used at the shaft seal, eye packing or at the balance drum. As Figure 1 shows, they are composed by a honeycomb surface stator inside which runs a rotor shaft that can be smooth or equipped with other type of seals, such as labyrinth, stepped or a second honeycomb pack.

The good performances of honeycomb seals in terms of leakage mass flow reduction and the enhanced rotor-dynamic stability have been evaluated first by Childs et al. (1989) after an experimental

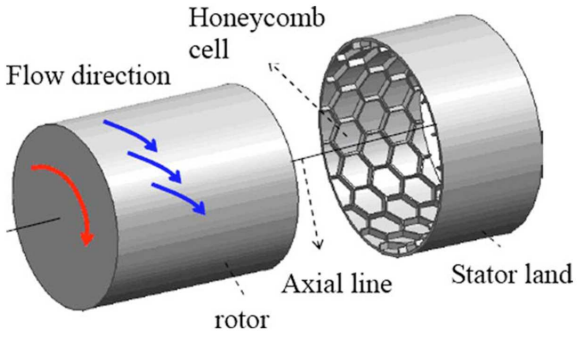


Figure 1: HONEYCOMB ANNULAR SEAL

investigation in which six types of honeycomb stators were analysed. Kleynhans (1996) developed a 1D code based on a constant temperature bulk-flow model, in order to estimate the friction factor for rotor-dynamic calculations of gas annular honeycomb seals. Chochua et al. (2002) performed a steady state CFD simulation on a seal composed by two honeycomb flat plates experimentally studied by Childs and Ha (1992). The results showed that flow structures developing inside the cells vary with clearance hydraulic diameter Reynolds number. Simulations were not capable to predict the friction factor jump phenomenon observed in the experiments. Keith et al. (2009) tried to explain the presence of friction factor jumps at different Reynolds numbers by an acoustic theory and proposed the use of the Strouhal number as the correct parameter to show the friction factor evolution.

Friction factor coefficient evaluation plays an important role not only for the prediction of seals leakages but also for its impact on seals rotor-dynamic characteristics. For this reason six different honeycomb seals configurations have been tested at Florence University on a stationary test rig. Obtained results have been used for leakage mass flow rate predictions in real seal configurations and compared with an experimental data-base provided by GE Oil & Gas obtaining a very good agreement as described in Micio et al. (2014). During such experimental campaign, friction factor jumps phenomena were observed and correlated by means of a correction to the Mach number, taking into account the different volume of cells and ducts, as previously proposed by Nakiboglu (2012). It was noticed that the friction factor jump was related to air system vibrations inside the seal: the flow overcoming the cells generates a forcing which can excite the air system. By reducing clearance dimensions the air system vibration is reduced and a damping of the friction factor damping is obtained.

In this work two additional intermediate clearances have been tested to extend the friction factor database. The acoustic interaction between the forcing generated by the flow overcoming the cells and the air system was deeply analysed through both experimental and numerical investigations. Hot wire anemometry was used to evaluate the forcing frequency and its evolution with main flow velocity, cell number and dimension while a FEM analysis was exploited for the air system eigenfrequencies calculation. These analyses permitted a clearer explanation of the phenomena leading to the friction factor jumps and their damping obtained for small clearances.

## EXPERIMENTAL FACILITY AND PROCEDURE

The stationary test rig designed with the help of a dedicated CFD analysis performed by Bianchini et al. (2013) and installed at the Industrial Engineering Department of University of Florence was exploited to carry out the measurement campaign.

This experimental investigation, aimed at measuring the pressure drops between the two plates

representing different honeycomb seals, was performed in order to create a data base of friction factor coefficients for each cell geometry (Massini et al. (2013) and Micio et al. (2014)).

The facility consists of an open loop suction type wind tunnel connected with the laboratory vacuum system composed of two vacuum pumps with a capacity of $900[m^3/h]$ each and two with $300[m^3/h]$ each as sketched in Figure 2.

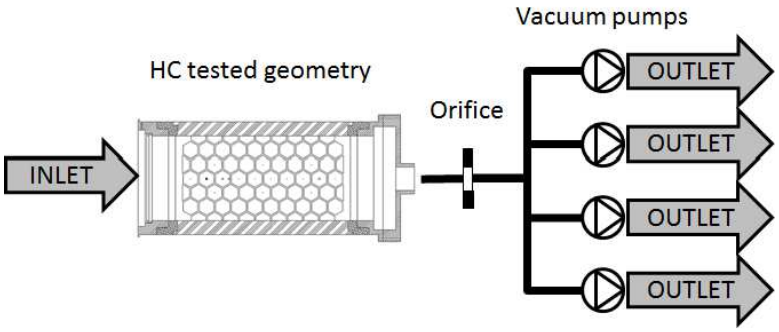


Figure 2: TEST RIG LAYOUT

A geometric scaling factor SF=30 was used to scale up the "honeycomb on smooth" seal having to improve confidence and accuracy on clearance dimensions. The test rig allows to reach realistic seals Mach number conditions, the maximum blowing capacity of employed vacuum pumps for air sucking limited achievable Reynolds number to a value lower than in real seals. Such value was however sufficient to reach the regime for which friction factor is almost independent from Reynolds number Bianchini et al. (2013).

Rotational effects were not reproduced as He et al. (2001) found out that only a small leakage reduction occurs for increasing rotational velocities. Furthermore a friction factor database provided by previous experimental campaigns performed on GE Oil & Gas rotating test rig was used for validation of leakage predictions on real seals. The discrepancies between measured mass flow leakages and predictions obtained by means of 1D codes, with friction factor values collected from measures presented in this work, were always below 20 % decreasing below 5% for $Re > 1.5E5$. Finally, it was found that the investigated acoustic phenomena can affect the friction factor coefficients providing an increase as high as 100%, see Micio et al. (2014) for details, with respect to which the effect of shaft rotation becomes negligible.

The sealing characterization is based on the friction factor distribution along the stream-wise direction, computed exploiting Equation 1:

$$f_f = \frac{D_h}{2}\frac{1}{M}\left(\frac{1-M^2}{(1+\frac{\gamma-1}{2}M^2)\gamma M^2}\right)\frac{dM}{dz} \tag{1}$$

Such equation is derived from the Fanno model (i.e. calorically perfect gas, steady and adiabatic flow, constant area duct, body forces and work crossing the control surface can be neglected). The Mach number gradient $\frac{dM}{dz}$ was evaluated using the central difference method $\left(\frac{dM}{dz}\right)_i = \left(\frac{M_{i+1}-M_{i-1}}{2\Delta z}\right)$ where subscripts "i" enumerate the pressure taps used for the calculation.

The Mach number is evaluated using equation 2 where $\dot{m}$ is the mass flow rate measured using a calibrated orifice downstream the test rig while $P$ is the static pressure measured using pressure taps disposed along the smooth plate in the stream wise direction. A flowchart of the complete post-processing procedure is presented in Figure 3.

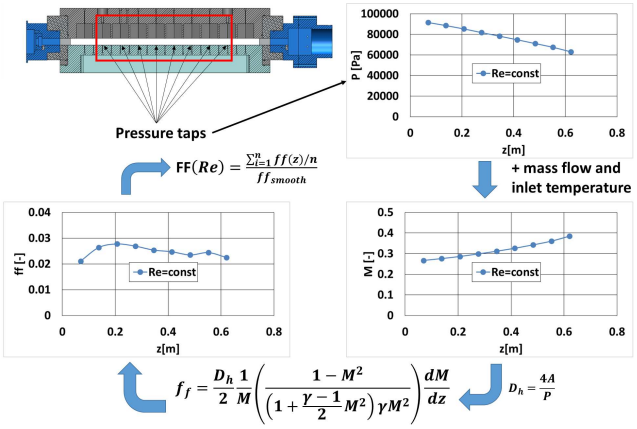


Figure 3: POST-PROCESSING FLOWCHART

$$M = \left( \frac{-1 + \sqrt{1 + 2(\gamma - 1)(\frac{\dot{m}}{PA})^2(\frac{RT_0}{\gamma})}}{\gamma - 1} \right)^{\frac{1}{2}} \tag{2}$$

The Reynolds number is calculated using the seal hydraulic diameter $Re = \rho c D_h / \mu$ resulting in a global investigated range from 40000 to 130000.

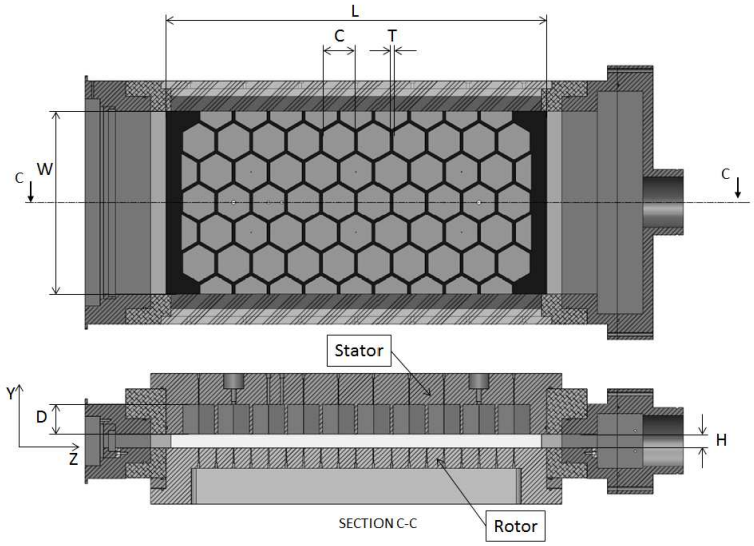


Figure 4: HONEYCOMB SEAL GEOMETRY

Six different geometries, each one tested with seven increasing clearances, were analyzed. Investigated geometrical parameters, cell width W, depth D, thickness T and orientation (i.e. which part of the cell faces the flow: the edge or the vertex of the hexagon) for the honeycomb cell and clearance H, are summarized in Table 1, scaled on the test section minimum clearance $H_0$, see Figure 4 for a clearer understanding of employed symbols.

| GEOMETRY | $C/H_0$ | $D/H_0$ | $T/H_0$ | $W/H_0$ | CELL ORIENTATION | $H/H_0$ |
|---|---|---|---|---|---|---|
| SMOOTH | \ | \ | \ | | \ | |
| GEO1 | 10.5 | 14 | 1 | | Vertex | |
| GEO2 | 10.5 | 14 | 1 | | Edge | |
| GEO3 | 10.5 | 10.8 | 1 | 58.3 | Edge | 1;1.25;1.5;2;2.5;3.5;4.5 |
| GEO4 | 10.5 | 9.67 | 1 | | Edge | |
| GEO5 | 8 | 13 | 0.4 | | Edge | |
| GEO6 | 8 | 8.82 | 0.4 | | Edge | |

Table 1: HONEYCOMB GEOMETRIES

**FRICTION FACTOR COEFFICIENTS**

The test rig validation was performed by comparing the pressure drops between two flat plates, "smooth on smooth" case, with Colebrook's correlation, explicitly reported in Equation 3 for the sake of clarity, as described in Massini et al. (2013).

$$\frac{1}{\sqrt{f_f}} = -2log\Big(\frac{\epsilon}{3.7D_h} + \frac{2.51}{Re_{D_h}\sqrt{f_f}}\Big) \tag{3}$$

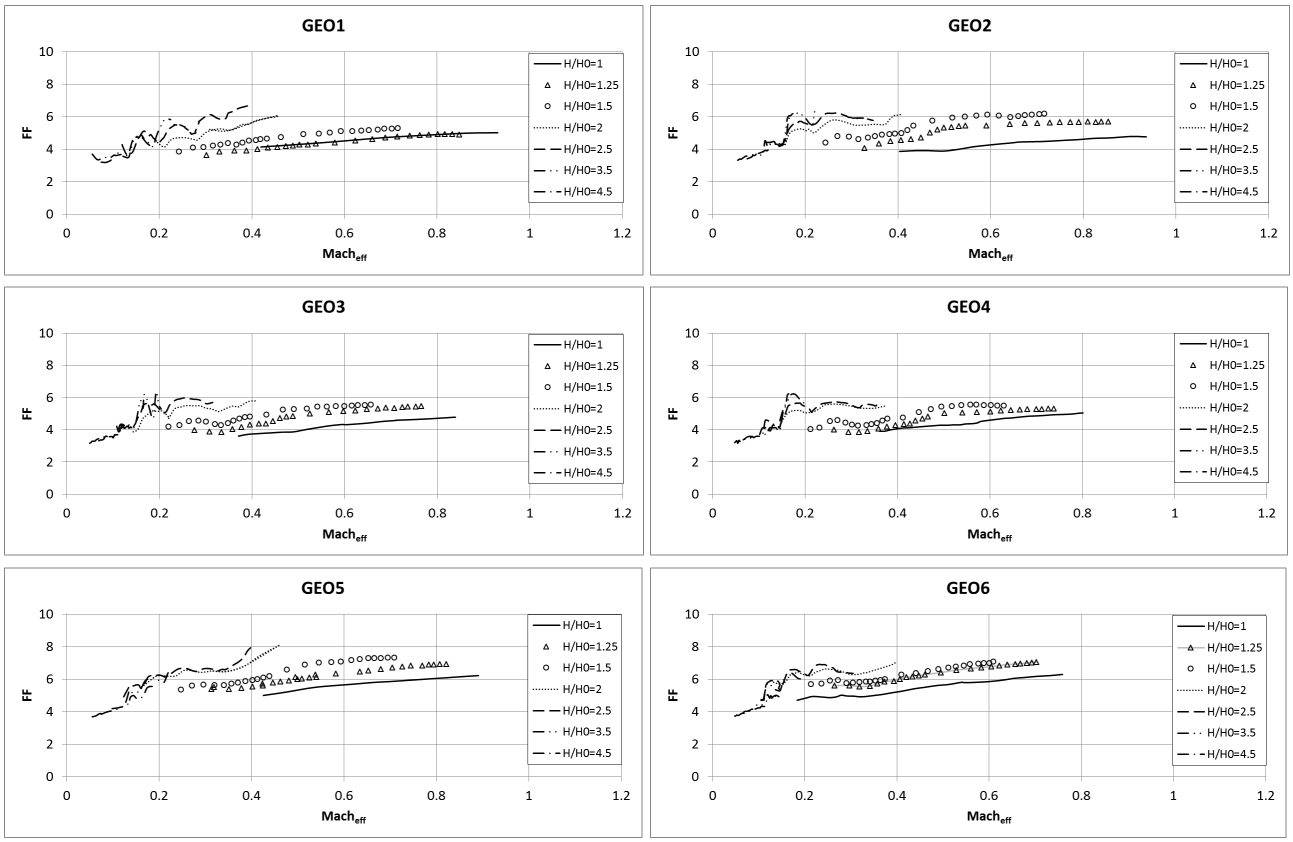


Figure 5: FRICTION FACTOR EVOLUTION WITH $M_{eff}$-ALL GEOMETRIES

Repeatability tests were also performed by monitoring the pressure drop both on the smooth and honeycomb side; the absence of hysteresis phenomena was also checked. The uncertainty analysis

follows the standard ASME (1985) based on Kline and McClintock (1953) method, resulting error is lower than 5% both for Reynolds and friction factor estimates, with an exception for the highest clearance in which, due to the very low pressure losses, the error can reach 15%.

Micio et al. (2014) showed that the presence of honeycomb seals provides a sensible increase of the average values of the friction factor compared to the "smooth on smooth" case. Analysing the friction factor evolution no monotonic trend was found neither varying the Reynolds number nor the clearance. In particular friction factor jumps occur at variable Reynolds number depending on the clearance.

Indeed it is well known that honeycomb seals are affected by flow acoustic interactions and the relevant parameter to represent the phenomenon responsible for the friction factor jumps is the Mach number. Nakiboglu (2012) suggested to correct the Mach number by changing the speed of sound to consider the additional air contained in the cells:

$$Mach_{eff} = M\sqrt{\frac{V_{tot}}{V_{duct}}} \tag{4}$$

where $V_{duct} = W \cdot L \cdot H$ and $V_{tot}$ is the overall volume of the seal (including cells).

Plotting the friction factor against the corrected Mach number $Mach_{eff}$ as in Figure 5, it is possible to note a slight rise of the $f_f$ with increasing $Mach_{eff}$ and the occurrence of friction factor jumps at certain distinct $Mach_{eff}$. A direct effect of the seal gap can be revealed from these plots as the jump amplitudes are damped for decreasing clearance. This behavior can be related to the higher air quantity that can be excited by acoustic resonance within the seal. In the following section this explanation will be discussed.

## ACOUSTIC RESULTS

In the preceding section the friction factor coefficients obtained from pressure measurements have been presented; in this section the interaction between rig acoustics and the aerodynamic forcing is further discussed to explain the onset of friction factor jumps.

Hot wire anemometry (HWA) was used to identify the forcing frequency due to the flow overcoming the cells. A 55P01 Dantec probe was positioned inside a cell close to the main flow duct: the effect of the probe within the gap was checked by varying its position both inside the honeycomb cell or in the middle of the channel obtaining the same results in terms of frequency peaks and friction factor coefficients, see Micio et al. (2014) for further details. The forcing frequency was found to be proportional to the Mach number inside the seal. This is in agreement with the well known Rossiter's formula based on semi empirical correlation, defining the Strouhal number for vortex shedding when a flow overcomes a cavity (Gloerfelt, 2009):

$$St = \frac{n - \alpha}{M + \frac{c}{U_c}}. \tag{5}$$

In Equation 5 $n$ is an integer number indicating the acoustic mode and $U_c$ is the convective velocity, i.e. the speed of the vortex moving inside the cavity, $\alpha$ is a constant parameter related to a time delay between the vortex arrival to the downstream wall and the emission of the acoustic pulse which is proportional to C/D.

Several suggestions may be found in literature, for example Gloerfelt (2009) proposed $\frac{U_c}{c} = 0.57$ and $\alpha = 0.25$ for a rectangular cavity with $C/D = 2$. Khanal et al. (2011) instead provided the relation $\alpha = 0.062\frac{C}{D}$ while Hassan et al. (2007) suggested that, when the Mach number is low and the cavity is deep, $\alpha$ is very close to zero. However, no specific values are available for honeycomb shaped cells. Due to the low shallow cavities considered in this work ($C/D < 1$, except for GEO4)

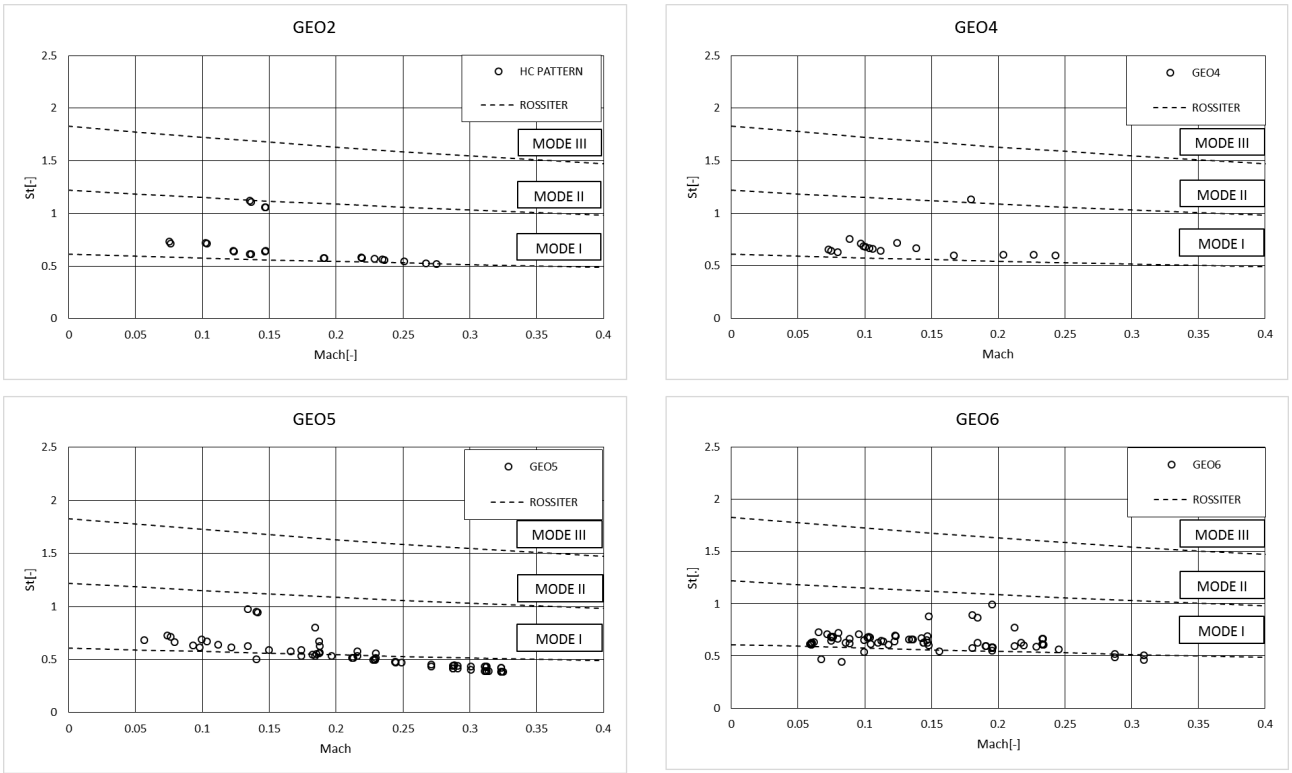


Figure 6: STROUHAL NUMBER FROM EXPERIMENT AND CORRELATION - GEO2, GEO4, GEO5, GEO6

and high acoustic speed compared to the bulk flow velocity ($M < 0.4$) best choice seemed to assume $\alpha = 0$. The second constant is finally set to the value that best fit obtained results, i.e. $\frac{U_c}{c} = 0.61$ as shown in Figure 6.

The presence of several points not collapsing on the correlation, suggested to deepen the analysis: in particular to verify possible occurrence of resonance phenomena within the rig. A modal unforced acoustic analysis of the test section was thus performed exploiting the FEM acoustic solver

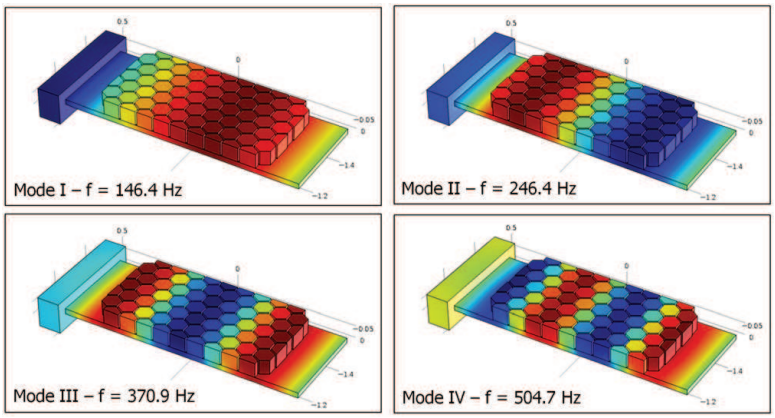


Figure 7: NUMERICAL EIGENMODES - GEO4

COMSOL®to identify natural eigenfrequencies and eigenmodes. Figure 7 depicts first four longitudinal eigenmodes obtained for GEO4 with intermediate clearance but, since modal shapes are not substantially affected by neither the honeycomb dimensions nor the clearance, such picture is qualitatively representative for all investigated geometries. Numerical eigenmodes are verified against

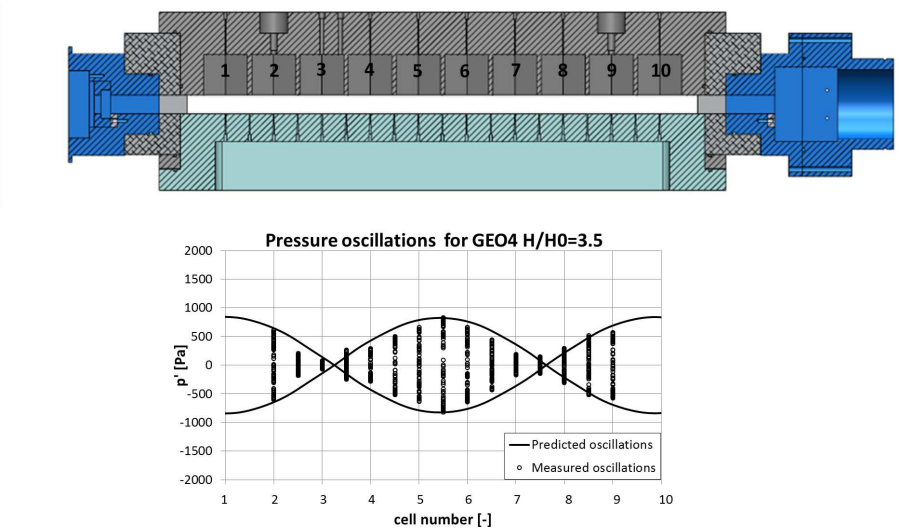


Figure 8: ACOUSTIC PRESSURE OSCILLATIONS

transient static pressure measurements which permitted to identify the position of acoustic nodes as depicted in Figure 8: static pressure oscillations were monitored at the flow speeds where friction factor jumps occur. It was so noticed that such oscillations have different amplitudes along the streamwise direction and can be zero where a pressure node is present. The number and the positions of the pressure nodes, as well as the qualitative behaviour of the fluctuation intensity, compared quite well with obtained FEM results.

The link between longitudinal modes and friction factor jumps is easily explained considering that, at constant bulk velocity, superposed pressure oscillations generate equivalent velocity fluctuations

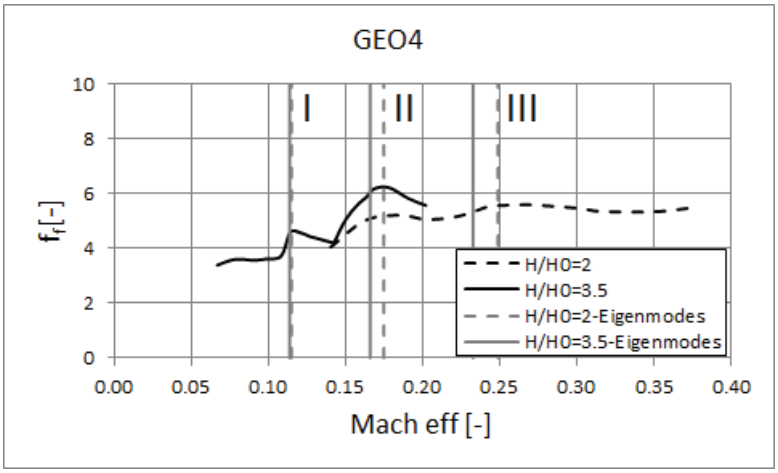


Figure 9: FRICTION FACTOR DISTRIBUTION - GEO4

which are responsible for higher pressure losses within the gap. Measured HWA principal frequencies showed in Figure 6 can be used to link the bulk velocity within the seal with the forcing frequencies generated by the cells. Thus, it is possible to estimate which is the air velocity able to excite the eigenfrequencies of the system predicted by the FEM calculations. Figure 9 clearly shows that the friction factor jumps occur when the velocity of the flow passing through the seal generates a forcing frequency close to the predicted eigenmodes of the system.

Geometry GEO2 was chosen for a further investigation aimed at understanding how many honeycomb cells represent the minimal periodic structure responsible for this oscillating behaviour. The entire honeycomb pattern was hence covered with tape isolating a single cell first, then a system of two and three adjacent cells. Figure 10 summarizes all the tests made comparing the reduced cells results, the honeycomb pattern and Rossiter's formula (dash line). Solid line is Strouhal number corresponding to the depth mode quarter wave frequency of the cavity, calculated using the following equation, Rayleigh (1896):

$$f_n = \frac{c}{4(D + 0.3C_{Dh})} \tag{6}$$

where $C_{Dh}$ is the hydraulic diameter of the cell section. The HWA frequency peaks, expressed in terms of Strouhal numbers in Figure 10, well collapse on Rossiter mode curves also for the reduced system investigations. Differently from the entire HC pattern, 1, 2 and 3 cells configurations show also higher modes as highlighted by the higher frequencies measured.

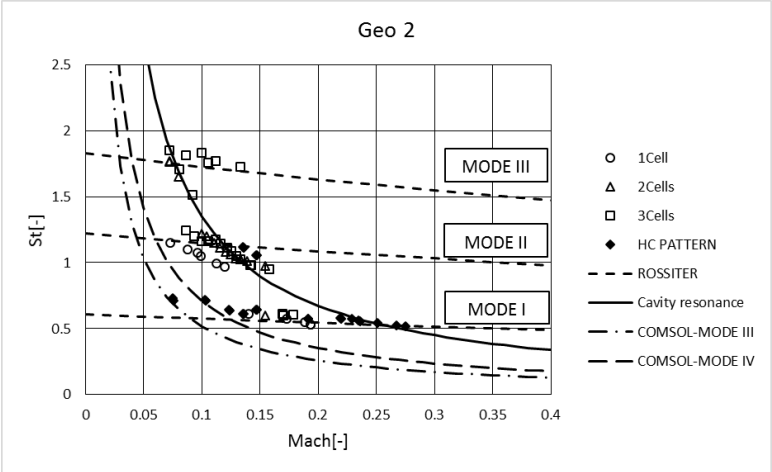


Figure 10: STROUHAL NUMBER FROM EXPERIMENT AND CORRELATION - GEO2 H/H0=2

Mode characterized by the largest fluctuation amplitudes is that closer to the cavity resonance curve; in fact lowest mode is registered at relatively high Mach only. Full HC pattern is instead showing first mode for the entire range of investigated Mach. This happens because of a higher energy of the aerodynamic forcing, due to the larger number of HC cells, which is sufficient to avoid interaction with cavity resonance. Furthermore such aerodynamic unsteadiness is capable of exciting the global acoustic behaviour of the rig. This occurs at low Mach number where acoustic eigenfrequencies of the entire rig match those of the forcing.

## CONCLUSIONS

An experimental investigation on the friction factor of flat plate honeycomb seals was performed. After a careful test rig validation six different honeycomb geometries were tested varying the Reynolds number between 40000 and 130000 and changing seven clearances.

Obtained friction factor distributions show several jumps occurring for each honeycomb geometry at the same corrected Mach number ($Mach_{eff}$) independently on the clearance. These increments in friction factor are due to acoustic phenomena developing within the seal.

With the aid of hot wire anemometry it was possible to identify the forcing frequency of the air stream over the honeycomb cells showing that it is proportional to the bulk flow velocity. When this frequency matches rig air system eigenfrequencies (detected by means of computational acoustic analysis), friction factor increases due to large pressure fluctuations within the seal. The magnitude of such fluctuations is proportional to the seal clearance. At small investigated clearances the damping is high enough that no friction factor jumps occurred.

## REFERENCES


ASME. Measurement uncertainty in instrument and apparatus. *vol. ANSI/ASME PTC 19.1-1985 of Performance Test Code, ASME*, (19), 1985.

C. Bianchini, M. Micio, F. Maiuolo, and B. Facchini. Numerical investigation to support the design of a flat plate honeycomb seal test rig. *ASME Turbo Expo*, (GT2013-95612), 2013.

D. W. Childs and T. W. Ha. Friction factor data for flat-plate tests of smooth and honeycomb surfaces. *ASME J. Tribol*, 114:722–730, 1992.

D. W. Childs and J. M. Vance. Annular gas seals and rotordynamics of compressors and turbines. *Proceedings of the* $26^{th}$ *Turbomachinery Symposium, Turbomachinery Laboratory, Texas A & M University, September 14-16, ASME, New York*, pages 201–220, 1997.

D. W. Childs, D. Elrod, and K. Hale. Annular honeycomb seals: Test results for leakage and rotordynamic coefficients; comparisons to labyrinth and smooth configurations. *ASME J. Tribol.*, 111: 293–300, 1989.

G. Chochua, W. Shyy, and J. Moore. Computational modeling for honeycomb-stator gas annular seal. *Int. J. Heat Mass Transfer*, 45:1849–1863, 2002.

X. Gloerfelt. Cavity noise. *VKI Lectures: Aeroacoustics of wall-bounded flow*, 2009.

M. El Hassan, L. Labraga, and L. Keirsbulck. Aero-acoustic oscillations inside large deep cavities. *Australian Fluid Mechanics Conference*, 2007.

L. He, X. Yuan, Y. Jin, and Z. Zhu. Experimental investigation of the sealing performance of honeycomb seals. *Chinese Journal of Aeronautics*, 14(1), 2001.

G. M. Keith, T. W. Ha, P. Bhattacharjee, D. W. Childs, K. K. Nielsen, and J. P. Platt. Friction factor jump in honeycomb seals explained by flow-acoustic interactions. *ASME Turbo Expo: Power of land, Sea and Air*, (GT2009-60337):1–8, 2009.

B. Khanal, K. Knowles, and A. J. Saddington. Computational study of flowfield characteristics in cavities with stores. *The aeronautical journal*, 1173(115), 2011.

G. F. Kleynhans. A two-control-volume bulk-flow rotordynamic analysis for smooth-rotor/honeycomb-stator gas annular seals, 1996.

S. J. Kline and F. A. McClintock. *Describing uncertainties in single sample experiments*. 1953.

D. Massini, B. Facchini, M. Micio, C. Bianchini, A. Ceccherini, and L. Innocenti. Analysis of flat plate honeycomb seals aerodynamic losses: effects of clearance. *Energy Procedia*, (ATI 2013-12282), 2013.

M. Micio, C. Bianchini, D. Massini, B. Facchini, A. Ceccherini, and L. Innocenti. Flat plate honeycomb seals friction factor analysis. *ASME Turbo Expo*, (GT2014-27078), 2014.

G. Nakiboglu. Aeroacoustics of corrugated pipes, 2012.

J. W. S. B. Rayleigh. *The theory of sound*, volume 2. Macmillan, 1896.